Acta Cryst. (1971). B27, 210

Crystal Structures in the $\{1\bar{3}2\}$ *CS* Family of Higher Titanium Oxides Ti_nO_{2n-1}

BY L. A. BURSILL AND B. G. HYDE

School of Chemistry, University of Western Australia, Nedlands, W.A. 6009, Australia

(*Received* 10 *March* 1970)

Electron microscopy/diffraction has been used to study the crystal structures of the family of titanium oxides Ti_nO_{2n-1}, $15 \leq n \lesssim 36$. Single-phase material does not occur; the structures are multiply twinned and show a wide variation in the degree of order. Thus X-ray studies failed to reveal these structures. Electron diffraction patterns are in excellent agreement with ideal unit-cell parameters based on a regular crystallographic shear operation $\frac{1}{2}[011]$ $(1\bar{3}2)$, (rutile) whereby one in every $2n$ oxygen-only $(1\bar{3}2)$ planes is eliminated from the rutile structure, and the adjacent rutile blocks closed up by the vector $\frac{1}{2}[011]$.

1. Introduction

In the stoichiometry range TiO_x, $1{\cdot}750 \leq x \leq 1{\cdot}889$, the existence of six ordered structures Ti_nO_{2n-1}, $4 \leq n \leq 9$, was revealed by X-ray powder diffraction (Andersson, Collén, Kuylenstierna & Magnéli, 1957). The structure of one of these, Ti_5O_9, was then determined by single-crystal X-ray diffraction analysis (Andersson, 1960). The 'ideal' Ti_5O_9 structure may be described as being derived from the 'idealized' rutile type (*cf.* § 2) by first removing every tenth oxygen-only plane parallel to $(1\bar{2}1)_r$,* and then displacing the adjacent rutile slabs by approximately $\frac{1}{2}[011]_r$ to collapse the structure. This restores the octahedral coordination of the titanium atoms and, across the crystallographic shear (*CS*) plane thus formed, the oxygen lattices are continuous but the titanium lattices are in antiphase. This model was then extended (to regular *CS* after removing every $2n$th oxygen-only plane) and successfully used to interpret the X-ray powder patterns of the other members of the series (Andersson & Jahnberg, 1963). It may be described as the regularly recurrent *CS* operation $\frac{1}{2}\langle 011\rangle$ $\{1\bar{2}1\}$, (rutile) (Anderson & Hyde, 1967). In the range $1{\cdot}89 \leq x \leq 2{\cdot}00$ X-ray powder diffraction analysis did not clearly reveal any further ordered phases, although it did suggest their existence (Andersson & Jahnberg, 1963).

By analogy with several ReO_3-derived series having *different CS* planes $\{1k0\}$, and noting the observation of discrete $\{1\bar{3}2\}$ planar faults in rutile by Eikum & Smallman (1965), Anderson & Hyde (1967) suggested that another family of titanium oxides probably existed. These would be derived by the regularly recurrent *CS* operation $\frac{1}{2}\langle 011\rangle$ $\{1\bar{3}2\}$, (rutile); and would also have the generic formula Ti_nO_{2n-1}. We believe that this is the family of phases recently reported (Bursill, Hyde, Terasaki & Watanabe, 1969). As with the earlier $\{1\bar{2}1\}$ family, their diffraction patterns showed a pronounced rutile-like substructure; but they also indicated that the *CS* planes were parallel to $\{1\bar{3}2\}_r$ and not $\{1\bar{2}1\}_r$. The observed values of n appeared to range from 15 to approximately 36 [but see § 4(*b*)], corresponding to TiO_x with $1{\cdot}933 \leq x \gtrsim 1{\cdot}972$. They were resolved by electron microscopy and selected area diffraction.

These $\{1\bar{3}2\}_r$ phases always exhibit fine scale polysynthetic twinning (Bursill *et al.*, 1969) and, in addition, several members coexist in all preparations [*cf.* § 4(*b*)]. Single-crystal X-ray diffraction analysis is therefore impossible. However, the hypothesis that the $\{1\bar{3}2\}_r$ family is derived by the regular *CS* operation $\frac{1}{2}\langle 011\rangle$ $\{1\bar{3}2\}$, (rutile) provides a plausible structural model on which to base an analysis of the available single-crystal electron diffraction patterns. The plausibility of this hypothesis is now substantially increased: we have determined that the displacement vector at an *isolated* $\{1\bar{3}2\}$ fault (a 'Wadsley defect', Andersson, 1970) in rutile is $\mathbf{R} \simeq \frac{1}{2}\langle 0, 0{\cdot}90, 0{\cdot}90\rangle_r$ and not $\frac{1}{6}\langle 211\rangle_r$ as suggested by van Landuyt (1966). This is very close to, and may be idealized as, $\frac{1}{2}\langle 011\rangle_r$ (Bursill & Hyde, 1970 *a*). Furthermore we have diffraction contrast evidence that this same displacement vector operates at parallel aligned $\{1\bar{3}2\}_r$ *CS* planes when they are aggregated into groups of 10 or so, with a mean separation of 4·5 to 5·0 nm (corresponding to $TiO_{\sim 1{\cdot}978}$) (Bursill & Hyde, 1970 *b*). These facts provide strong support for the proposed model.

We therefore assume that the displacement vector at ordered $(1\bar{3}2)_r$ *CS* planes is the same, *viz.* $\mathbf{R} \simeq \frac{1}{2}[011]_r$. This allows us to deduce unit-cell parameters for the ordered $(1\bar{3}2)_r$ phases which are in excellent agreement with the observed diffraction patterns.

2. The structural model

Rutile (TiO_2) is tetragonal ($a_r = 0{\cdot}45937$, $c_r = 0{\cdot}29581$ nm) with Ti at 000 and $\frac{1}{2}\frac{1}{2}\frac{1}{2}$, and O at $uu0$; $\bar{u}\bar{u}0$; $\frac{1}{2}-u$, $\frac{1}{2}+u$, $\frac{1}{2}$; $\frac{1}{2}+u$, $\frac{1}{2}-u$, $\frac{1}{2}$; and $u = 0{\cdot}305$ (Wyckoff, 1963). The oxygen atoms are in a puckered hexagonal close packed arrangement, the titanium atoms occupying alternate rows of octahedral interstices parallel to $\mathbf{c}_r \equiv \mathbf{a}_{hex}$. If the rutile structure is idealized so that $u =$

* The subscript r denotes rutile indices.

0·25 then $\frac{1}{2}[011]_r$ is a vector in the oxygen lattice, but goes from a titanium-filled row of octahedral interstices to an empty row.

Fig. 1(*a*) and (*b*) shows the idealized layers at $z_r=0,\frac{1}{2}$ after removing every eighteenth oxygen-only plane parallel to $(1\bar{3}2)_r$ and closing up adjacent rutile slabs by a mutual displacement equal to the 'ideal' vector $\mathbf{R}=\frac{1}{2}[011]_r$. The structure along the *CS* plane resembles that in the $(1\bar{2}1)_r$ family, except that the face-sharing octahedra are 50 per cent further apart (*cf.* Figs. 6 and 12 of Anderson & Hyde, 1967). In the idealized rutile structure the sequence of atom planes parallel to $(1\bar{3}2)$ is

$$\cdots\mathbf{B}\,\mathbf{A}\,\mathbf{B}\,\mathbf{A}\,\mathbf{B}\,\mathbf{A}\,\mathbf{B}\,\mathbf{A}\,\mathbf{B}\cdots$$

($\mathbf{A}$=TiO, $\mathbf{B}$=O). The presence of a *CS* plane (.) modifies this to

$$\cdots\mathbf{B}\,\mathbf{A}\,\mathbf{B}\,\mathbf{A}\,.\,\mathbf{A}\,\mathbf{B}\,\mathbf{A}\,\mathbf{B}\cdots$$

The modular unit between *CS* planes is $n\mathbf{A}+(n-1)\mathbf{B}$, giving the same generic formula, Ti_nO_{2n-1}, as for the $(1\bar{2}1)_r$ family.

Consideration of the three-dimensional lattices occupied by the face-sharing pairs of $[TiO_6]$ octahedra for different n values leads to the following axial systems for the Ti_nO_{2n-1} $(1\bar{3}2)_r$ structures in terms of the rutile-type substructures.

(i) For *even* values of n:

$$\mathbf{a}=2\mathbf{a}_r-\mathbf{c}_r\,,$$
$$\mathbf{b}=-\mathbf{a}_r-\mathbf{b}_r-\mathbf{c}_r\,,$$
$$\mathbf{c}=\mathbf{a}_r-\tfrac{5}{2}\mathbf{b}_r+(n-9)/2\mathbf{c}_r\,.$$

(ii) For *odd* values of n:

$$\mathbf{a}=\mathbf{a}_r-\mathbf{b}_r-2\mathbf{c}_r\,,$$
$$\mathbf{b}=\mathbf{a}_r+\mathbf{b}_r+\mathbf{c}_r\,,$$
$$\mathbf{c}=-\tfrac{5}{2}\mathbf{b}_r+(n-8)/2\mathbf{c}_r\,.$$

Different systems for even and odd n are necessary in order to have primitive unit-cells with reasonably short c axes. An alternative choice would be to double the c axes for odd n. (*cf.* Andersson & Jahnberg doubled the c axes of Ti_nO_{2n-1} $(1\bar{2}1)_r$ for even n.) However this is confusing as it leads to non-primitive unit cells.

The 'ideal' unit-cell parameters for $15\leq n\leq 22$ are given in Table 1. The following direct matrices relate the indices of rutile and Ti_nO_{2n-1} $(1\bar{3}2)_r$ reflexions.

(i) n even:

Ti_nO_{2n-1} $(1\bar{3}2)_r$	rutile		
	2	0	$\bar{1}$
	$\bar{1}$	$\bar{1}$	$\bar{1}$
↓	1	$-\frac{5}{2}$	$(n-9)/2$

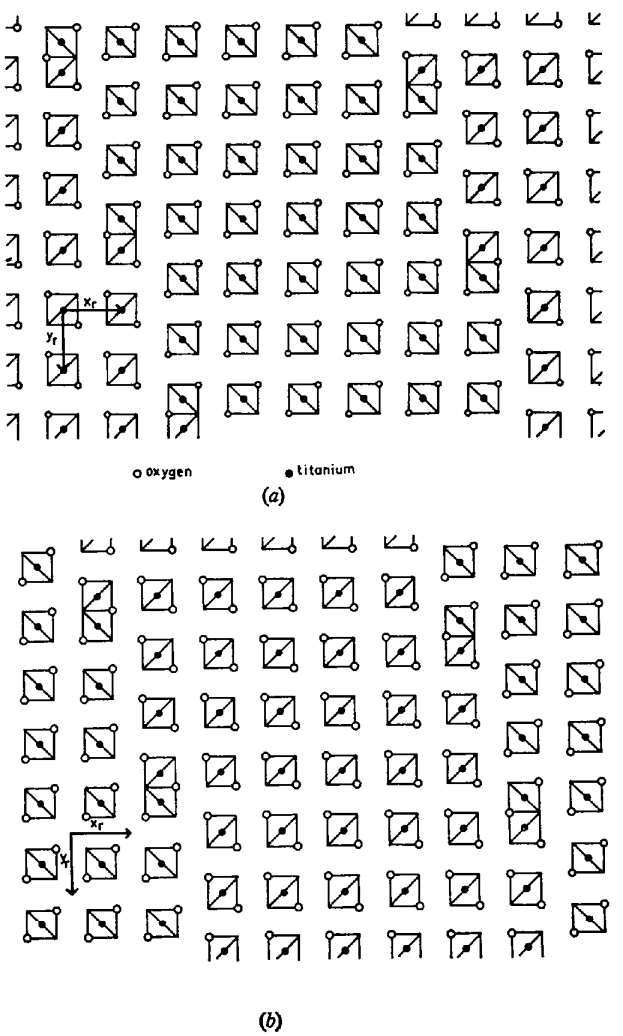

Fig. 1. Idealized ($u=0{\cdot}25$) layers parallel to $(001)_r$ after removing every eighteenth oxygen-only plane parallel to $(1\bar{3}2)_r$ and closing up the adjacent rutile slabs by $\mathbf{R}=\frac{1}{2}[011]_r$. (*a*) $z_r=0$; (*b*) $z_r=\frac{1}{2}$.

Table 1. *'Ideal' unit-cell parameters of* $(1\bar{3}2)_r$ *CS structures*

n	a	b	c	α	β	γ
15	0·87867 nm	0·71382 nm	1·54622 nm	101·57°	93·58°	106·20°
16	0·96519	0·71382	1·61302	89·49	85·73	119·05
17	0·87867	0·71382	1·75808	96·12	99·69	106·20
18	0·96519	0·71382	1·81710	93·41	89·07	119·05
19	0·87867	0·71382	1·99145	91·87	104·39	106·20
20	0·96519	0·71382	2·04374	96·48	91·72	119·05
21	0·87867	0·71382	2·23962	88·52	108·06	106·20
22	0·96519	0·71382	2·28625	98·90	93·81	119·05

(ii) n odd

	rutile		
Ti_nO_{2n-1} $(1\bar{3}2)_r$	1	$\bar{1}$	$\bar{2}$
	1	1	1
↓	0	$-\frac{5}{2}$	$(n-8)/2$

The following inverse matrices may be used to calculate the 'ideal' atomic coordinates x, y, z of a Ti_nO_{2n-1} $(1\bar{3}2)_r$ homologue from the rutile coordinates x_r, y_r, z_r.

(i) n even:

		Ti_nO_{2n-1} $(1\bar{3}2)_r$		
rutile	$1/(2n-1)$	$n-4$	$\bar{5}$	2
		$11-n$	$16-2n$	$\bar{6}$
↓		$\bar{7}$	$\bar{10}$	4

(ii) n odd:

		Ti_nO_{2n-1} $(1\bar{3}2)_r$		
rutile	$1/(2n-1)$	$n-3$	$n+2$	2
		$8-n$	$n-8$	$\bar{6}$
↓		$\bar{5}$	5	4

3. Specimen preparation

Six samples were prepared under the conditions set out in Table 2. The single-crystal starting material was from a boule of approx 99·8 per cent purity supplied by Nakazumi Crystals Corporation (Osaka, Japan). Powder samples were prepared from Koch–Light's 99·9 per cent rutile.

Electron microscope specimens were made by crushing the powder or small chips of single crystal between glass slides, and mounting the fracture flakes on carbon support films. They were examined in a JEM-6A microscope operated at 100 kV, and could be tilted up to ±20° about any horizontal axis.

4. Experimental results and their interpretation

(*a*) *Indexing the diffraction patterns*

Examples of diffraction patterns showing closely spaced reflexions along $\mathbf{g}(1\bar{3}2)_r$ and/or $\mathbf{g}(1\bar{2}1)_r$ are given in Figs. 2 to 7. They may only be unambiguously indexed (and hence a reliable value assigned to n) for symmetrically-excited low order Laue zones with the *CS* planes parallel to the incident beam, and well ordered. The strong reflexions lie close to rutile positions: those close to the $\{132\}_r$ and/or $\{121\}_r$ positions (and lying along the rows of closely-spaced spots produced by the ordered *CS* planes) are indexed as $(1\bar{3}2)_r$ and/or $(1\bar{2}1)_r$ respectively. The other strong reflexions are then indexed (also as rutile spots) and the corresponding rutile zone axis determined.

The displacement vector $\frac{1}{2}[011]_r$ has collapse components of $0{\cdot}50d_{1\bar{3}2}$ and $0{\cdot}50d_{1\bar{2}1}$ normal to $(1\bar{3}2)_r$ and $(1\bar{2}1)_r$ respectively, *i.e.* the *ideal CS* spacings are $D_{1\bar{3}2}=d_{1\bar{3}2}(n-0{\cdot}50)$ and $D_{1\bar{2}1}=d_{1\bar{2}1}(n-0{\cdot}50)$, with $d_{1\bar{3}2}=0{\cdot}1036$ and $d_{1\bar{2}1}=0{\cdot}1687$ nm. From these equations an approximate value for n may be deduced by measuring the interval between the closely-spaced spots along $\mathbf{g}(1\bar{3}2)_r$ and/or $\mathbf{g}(1\bar{2}1)_r$.

The rutile zone axis is then transformed to the corresponding Ti_nO_{2n-1} zone axis by using the inverse matrix given above for the (1$\bar{3}$2) structures, or the similar matrices given by Andersson & Jahnberg (1963) for (1$\bar{2}$1) structures. *N.B.* The matrices only apply for (1$\bar{3}$2) and (1$\bar{2}$1) *CS* planes, and not for {1$\bar{3}$2} and {1$\bar{2}$1} without appropriate permutations. A detailed comparison of observed and calculated d spacings and interplanar angles for several adjacent n values (using the unit-cell parameters given in Table 1 for the (1$\bar{3}$2) phases and those of Andersson & Jahnberg (1963) for the (1$\bar{2}$1) phases) then establishes n uniquely. Table 3 gives the results of such a comparison for several n values in both series: the agreement between the observed and calculated values is well within experimental error. Uncertainties in the camera constant, and streaking through the diffraction spots, may

Table 2. *Preparation conditions and compositions of samples*

Sample No.(*a*)	Method of preparation(*b*)	Preparation temperature(*c*) K	Time (days)	Ratio p_{H_2}/p_{H_2O}	Estimated composition(*d*) $\bar{x}$
1*s*	*A*	1343	6	30	1·96 *i*
2*s*	*A*	1223	2	300	1·94–5 *i*
3*s*	*A*	1245	3	300	1·936 *j*
4*s*	*A*	1275	4	300	1·9268 *k*
5*s*	*A*	1275	4	300	1·9247 *k*
6*p*	*B*	1303	?	?	1·889 *l*

(*a*) *s*=single crystal; *p*=powder.
(*b*) TiO_2 reduced by either *A*, equilibrating with a flowing H_2+H_2O gas mixture in a tube furnace, or *B*, equilibrating with a circulating H_2+H_2O gas mixture, the sample being on a microbalance.
(*c*) All samples were cooled to room temperature in about 15 minutes.
(*d*) Composition determined by
i estimation, using p_{H_2}/p_{H_2O} *vs.* $\bar{x}$ data from R. R. Merritt (unpublished). Accuracy, $\Delta\bar{x}\simeq\pm0{\cdot}005$.
j weighing approx 2g of sample before and after reduction; $\Delta\bar{x}\simeq\pm0{\cdot}001$.
k reoxidising approx 0·5g of sample to TiO_2 in O_2 on an Ainsworth thermobalance; $\Delta\bar{x}\simeq\pm0{\cdot}0002$.
l measuring the weight loss of a TiO_2 sample on a Cahn thermobalance; $\Delta\bar{x}\simeq\pm0{\cdot}0005$.

Figs. 2 to 7. Examples of indexed diffraction patterns of $(1\bar{2}1)_r$ and $(1\bar{3}2)_r$ *CS* phases.

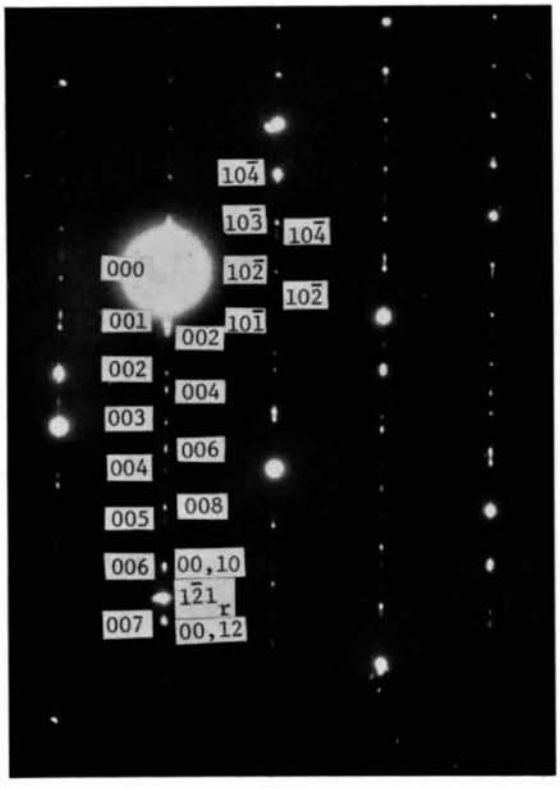

Fig. 2. $n=6,7(1\bar{2}1)_r$, zone axis [010].

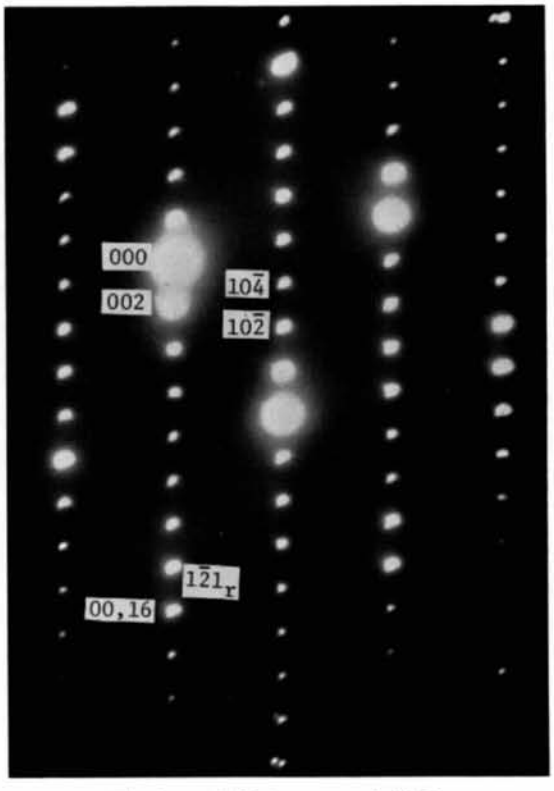

Fig. 3. $n=8(1\bar{2}1)_r$, zone axis [010].

[*To face p.* 212

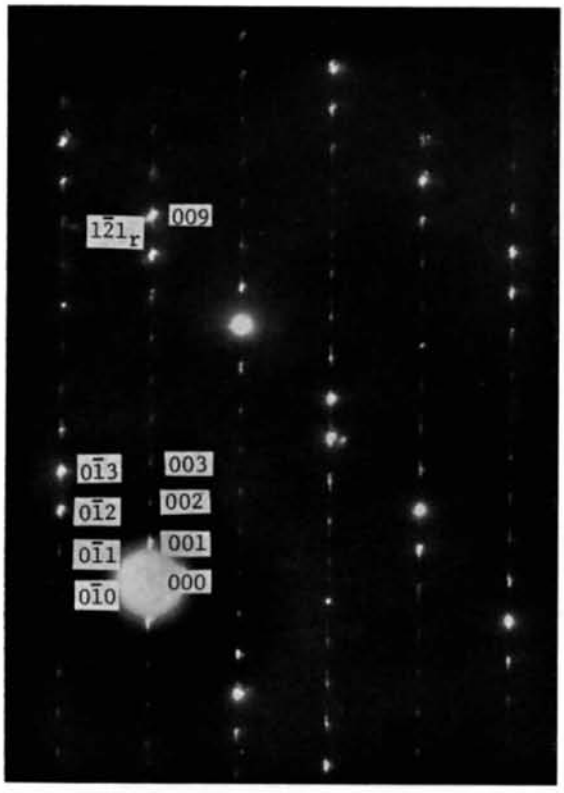

(a)

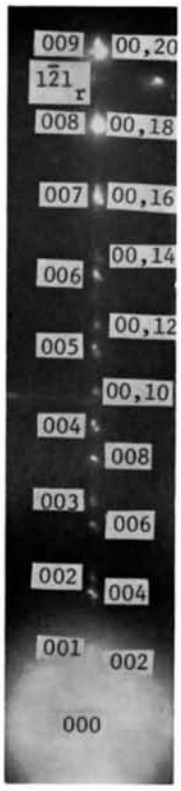

(b)

Fig. 4. (a) $n=9(1\bar{2}1)_r$, zone axis [100]. (b) $n=9,10(1\bar{2}1)_r$, (00l) row.

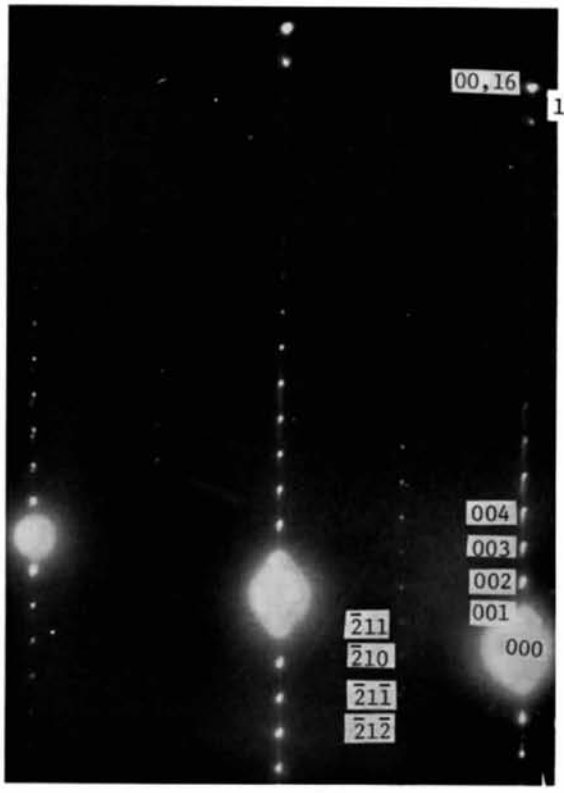

Fig. 5. $n=16(1\bar{3}2)_r$, zone axis [120].

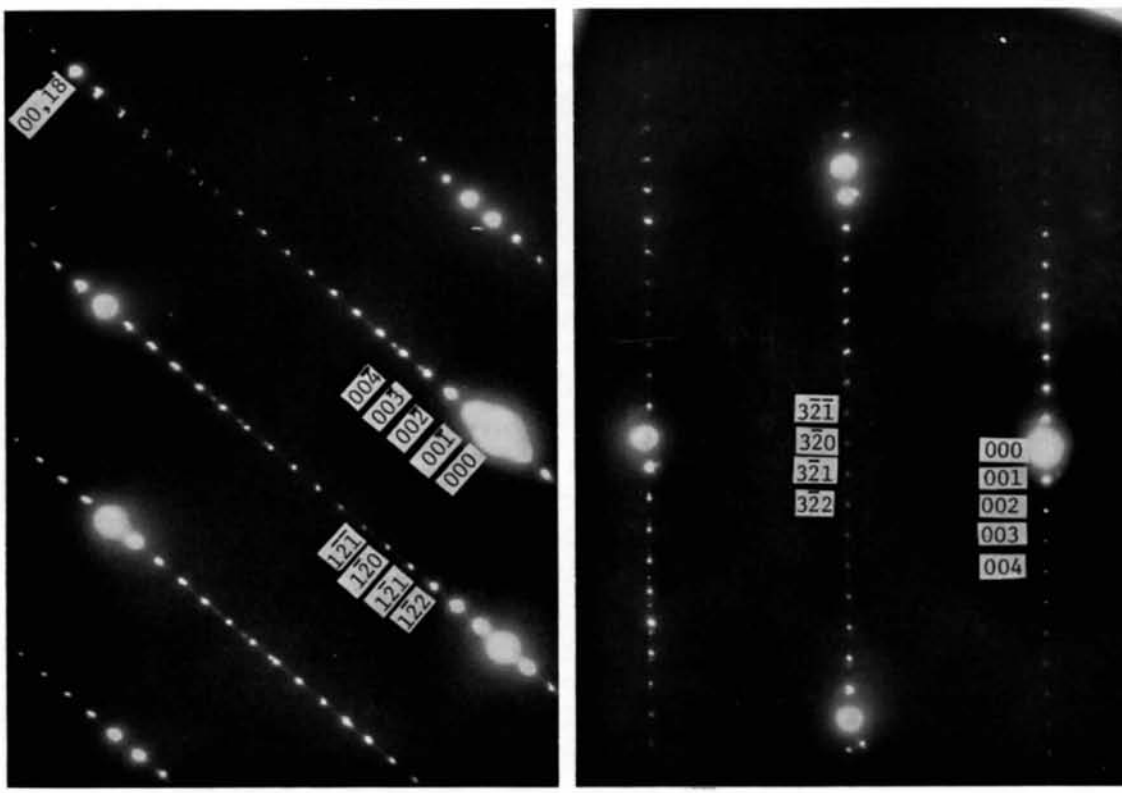

(*a*) (*b*)

Fig. 6. (*a*) $n=18(1\bar{3}2)_r$, zone axis [210]. (*b*) $n=18(1\bar{3}2)_r$, zone axis [230].

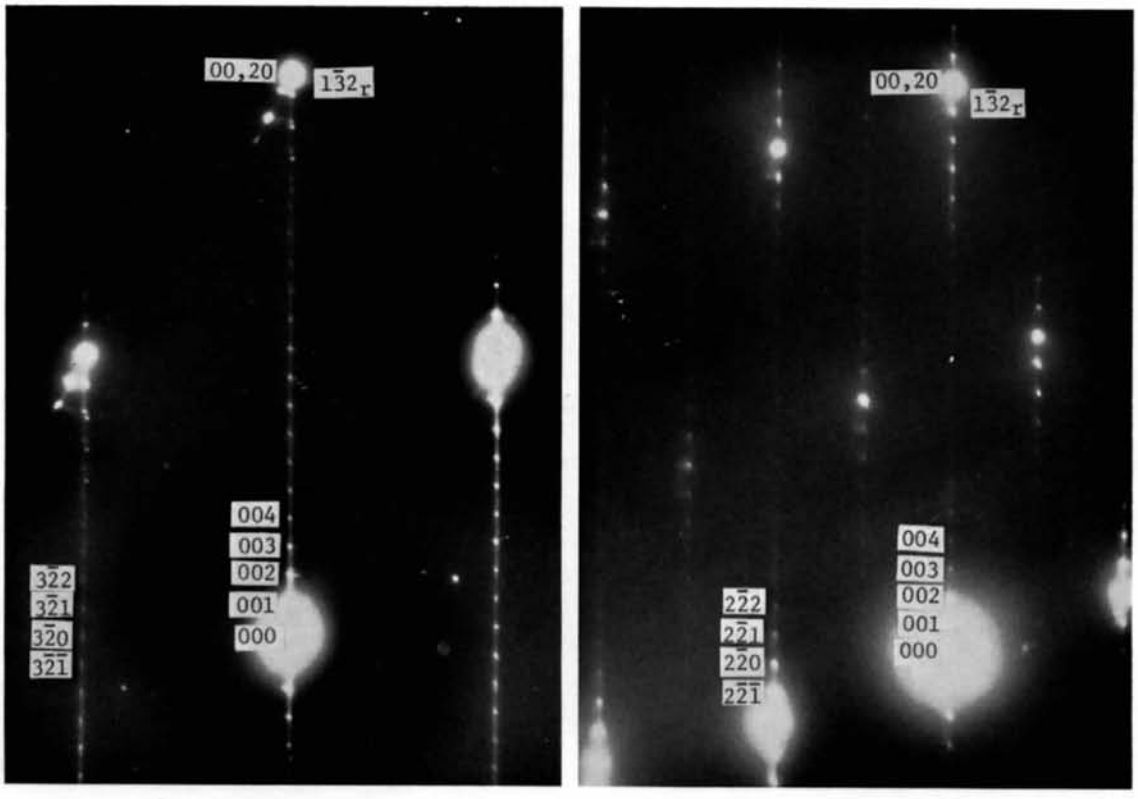

(*a*) (*b*)

Fig. 7. (*a*) $n=20(1\bar{3}2)_r$, zone axis [230]. (*b*) $n=20(1\bar{3}2)_r$, zone axis [110].

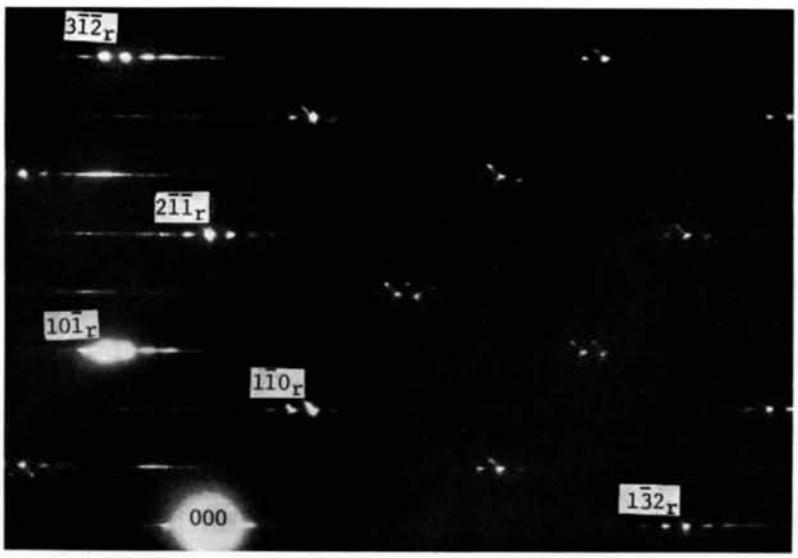

(*a*)

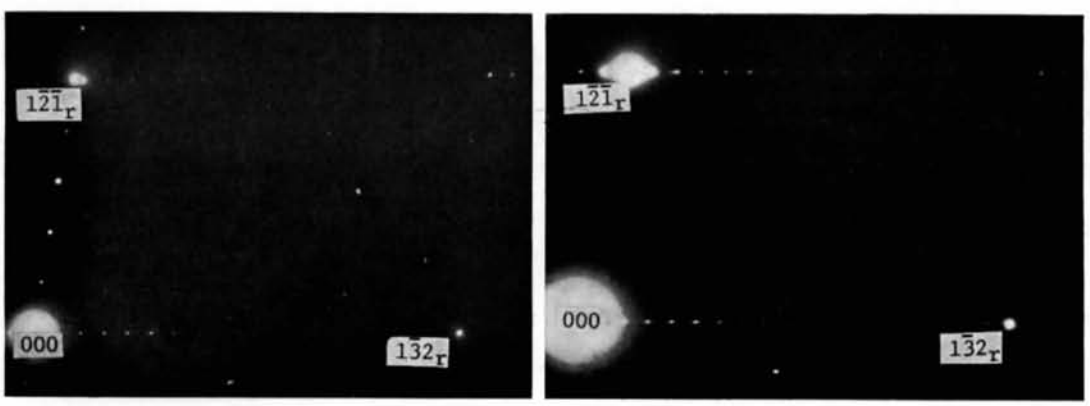

(*b*) (*c*)

Fig. 8. (*a*) Diffraction pattern of a disordered specimen of $n \simeq 25(1\bar{3}2)_r$ showing streaking parallel to $g(1\bar{3}2)_r$. Note that this intersects $g(2\bar{1}\bar{1})_r$ 5 times, $g(3\bar{1}2)_r$ 8 times, $g(10\bar{1})_r$ 3 times and $g(1\bar{1}0)_r$ 2 times. (*b*) Diffraction pattern of a well ordered specimen of $n = 18(1\bar{3}2)_r$ with 5 'spots' along $g(12\bar{1})_r$ arising from the twin orientation with $(3\bar{1}2)_r$ *CS* planes inclined at 60·6° to the incident beam. (*c*) Diffraction pattern from an area adjacent to that which gave (*b*); twin orientation now absent.

make it difficult to establish n to better than ± 1 if $n \gtrsim 20$.

The importance of specimen orientation and order is illustrated by Fig. 8(*a*) in which it is clear that streaking parallel to $\mathbf{g}(1\bar{3}2)_r$ intersects $\mathbf{g}(2\bar{1}\bar{1})_r$ five times, $\mathbf{g}(3\bar{1}\bar{2})_r$ eight times, $\mathbf{g}(10\bar{1})_r$ three times and $\mathbf{g}(1\bar{1}0)_r$ twice. When this streaking is inclined to the reflecting sphere it will produce apparently sharp reflexions along these reciprocal lattice vectors. Continuous streaking parallel to $\mathbf{g}(1\bar{3}2)_r \equiv \mathbf{g}(00L)$ means that there is scattered intensity for $\mathbf{g}(HKL)$ with *all*, including non-integral, values of L. (H, K and L are indices in the Ti_nO_{2n-1} system). The number of 'spots' along $\mathbf{g}(hkl)_r$ is therefore equal to the highest common factor of H and K. Thus in the above example

$(2\bar{1}\bar{1})_r$ transforms to $(5, 0, 9-\frac{1}{2}n)_i$ or $(5, 0, 6\frac{1}{2}-\frac{1}{2}n)_{ii}$;
$(3\bar{1}\bar{2})_r$ transforms to $(8, 0, 14\frac{1}{2}-n)_i$ or $(8, 0, 10\frac{1}{2}-n)_{ii}$;
$(10\bar{1})_r$ transforms to $(3, 0, 5\frac{1}{2}-\frac{1}{2}n)_i$ or $(3, 0, 4-\frac{1}{2}n)_{ii}$;
$(1\bar{1}0)_r$ transforms to $(2, 0, 3\frac{1}{2})_i$ or $(2, 0, 2\frac{1}{2})_{ii}$;

and so we expect 5, 8, 3 and 2 spots respectively along $\mathbf{g}(2\bar{1}\bar{1})_r$, $\mathbf{g}(3\bar{1}\bar{2})_r$, $\mathbf{g}(10\bar{1})_r$ and $\mathbf{g}(1\bar{1}0)_r$.

In addition to the 18 spots along $\mathbf{g}(1\bar{3}2)_r$, due to the ordered $(1\bar{3}2)_r$ *CS* planes parallel to the incident beam, Fig. 8(*b*) shows 5 'spots' along $\mathbf{g}(1\bar{2}1)_r$. $(1\bar{2}1)_r$ transforms to $(3, 2, 10\frac{1}{2}-\frac{1}{2}n)_i$ or $(5, \bar{2}, 9-\frac{1}{2}n)_{ii}$; so that no intermediate spots are expected to appear along $\mathbf{g}(1\bar{2}\bar{1})_r$. This apparent anomaly is simply explained by assuming the presence of $(3\bar{1}2)_r$ *CS* planes (inclined at 60·6° to the incident beam), *i.e.* the crystal is twinned. The reflexion $(1\bar{2}\bar{1})_r$ then transforms to $(5, 0, 9-\frac{1}{2}n)_i$ or $(5, 0, 6\frac{1}{2}-\frac{1}{2}n)_{ii}$ in the twin system. In this particular case they would be expected even for a perfectly ordered perfectly oriented crystal since, for $n=18$, $(1\bar{2}\bar{1})_r \rightarrow (500)_t$. Many similarly twinned patterns were en-

Table 3. *d spacings and interplanar angles in* $(1\bar{2}1)_r$ *and* $(1\bar{3}2)_r$ *CS structures; a comparison of observed values with those calculated from the direct matrices in Andersson & Jahnberg* (1963) (*for* $(1\bar{2}1)_r$) *and in this paper* (*for* $(1\bar{3}2)_r$)

Plate number	Figure number	*CS* plane	n	Zone axis Ti_nO_{2n-1} indices	(HKL)	d_{HKL} Obs.	d_{HKL} Calc.	$(00L)\wedge(HKL)$ Obs.	$(00L)\wedge(HKL)$ Calc.
8049	2	$(1\bar{2}1)$	6	[010]	002	0·955 nm	0·9546 nm		
					$10\bar{2}$	0·518	0·5180	79·5°	79·25°
					100	0·423	0·4234	53·5	53·42
					$10\bar{4}$	0·491	0·4957	110·0	109·93
					102	0·321	0·3232	38·0	37·69
			7	[010]	001	1·123	1·1235		
					$10\bar{2}$	0·524	0·5252	92·0	91·56
					$10\bar{1}$	0·483	0·4808	67·0	66·24
					100	0·394	0·3890	47·5	47·76
					$10\bar{3}$	0·467	0·4709	117·0	116·33
8078	3	$(1\bar{2}1)$	8	[010]	002	1·297	1·2984		
					$10\bar{4}$	0·511	0·5129	78·5	77·83
					$10\bar{2}$	0·448	0·4460	58·5	58·21
					100	0·366	0·3666	44·0	44·32
					102	0·302	0·3010	34·5	35·00
5213	4(*a*)	$(1\bar{2}1)$	9	[100]	001	1·452	1·460		
					$0\bar{1}2$	0·631	0·6249	71·5	70·43
					$0\bar{1}1$	0·667	0·6647	97·0	95·72
					$0\bar{1}0$	0·578	0·5834	120·0	119·14
					$0\bar{1}3$	0·518	0·5178	50·5	50·83
5215	4(*b*)	$(1\bar{2}1)$	10	[100]	002	1·595	1·6007		
7012	5	$(1\bar{3}2)$	16	[120]	001	1·611	1·6064		
		$\frac{1}{2}[011]$			$\bar{2}10$	0·472	0·4706	86·5	86·45
					$\bar{2}1\bar{1}$	0·458	0·4594	103·0	103·03
					$\bar{2}11$	0·444	0·4443	70·5	70·43
					$\bar{2}1\bar{2}$	0·417	0·4175	117·8	117·70
		$\frac{1}{6}[121]$			001	1·611	1·6064		
					$\bar{2}10$	0·472	0·4715	86·5	89·26
					$\bar{2}1\bar{1}$	0·458	0·4540	103·0	105·67
					$\bar{2}11$	0·444	0·4508	70·5	72·96
					$\bar{2}1\bar{2}$	0·417	0·4089	117·8	119·86
7345	6(*a*)	$(1\bar{3}2)$	18	[210]	001	1·823	1·814		
		$\frac{1}{2}[011]$			$1\bar{2}0$	0·354	0·3532	92·5	93·49
					$1\bar{2}1$	0·348	0·3507	81·2	82·36
					$1\bar{2}\bar{1}$	0·344	0·3428	103·2	104·36
					$1\bar{2}2$	0·335	0·3361	70·7	71·78
		$\frac{1}{6}[121]$			001	1·823	1·814		
					$1\bar{2}0$	0·354	0·3523	92·5	95·35
					$1\bar{2}1$	0·348	0·3520	81·2	84·21
					$1\bar{2}\bar{1}$	0·344	0·3399	103·2	106·10
					$1\bar{2}2$	0·335	0·3392	70·7	73·48

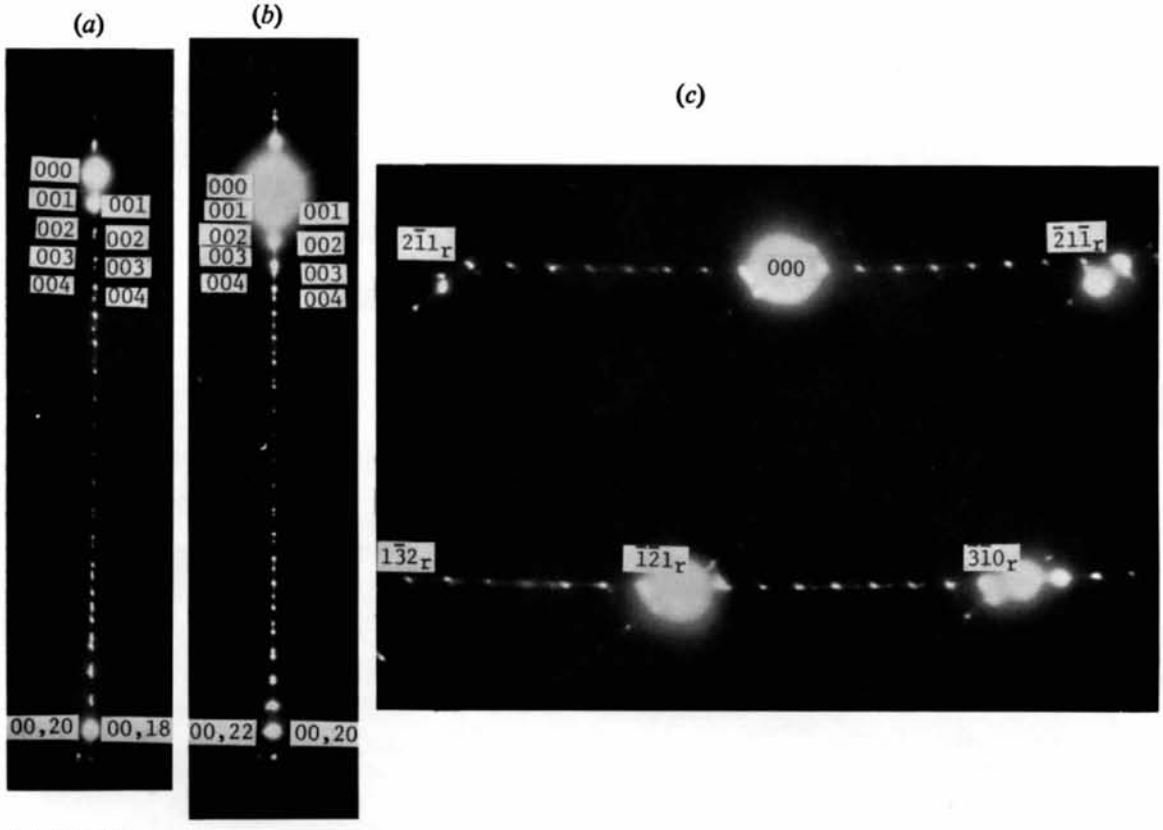

Fig.9. (*a*), (*b*) Diffraction patterns of $(1\bar{3}2)_r$ *CS* phase mixtures showing a parallel intergrowth of (*a*) $n=18$, 20; (*b*) $n=20$, 22; [(00*l*) rows]. (*c*) Diffraction pattern from a mixture of $n=9$, $10(1\bar{2}1)_r$ and $n=16(1\bar{3}2)_r$.

[*To face p.* 213

Table 3 (*cont.*)

Plate number	Figure number	*CS* plane	*n*	Zone axis Ti_nO_{2n-1} indices	(*HKL*)	d_{HKL} Obs.	d_{HKL} Calc.	(00*L*) ∧ (*HKL*) Obs.	(00*L*) ∧ (*HKL*) Calc.
7377	6(*b*)	(1$\bar{3}$2)	18	[230]	001	1·833	1·814		
		½[011]			3$\bar{2}$0	0·289	0·2903	92·0	92·30
					3$\bar{2}$1	0·288	0·2885	83·0	83·15
					3$\bar{2}$$\bar{1}$	0·285	0·2849	100·7	101·33
					3$\bar{2}$2	0·279	0·2798	74·0	74·34
		⅛[121]			001	1·833	1·814		
					3$\bar{2}$0	0·289	0·2905	92·0	90·76
					3$\bar{2}$1	0·288	0·2875	83·0	81·64
					3$\bar{2}$$\bar{1}$	0·285	0·2863	100·7	99·84
					3$\bar{2}$2	0·279	0·2777	74·0	72·93
6741	7(*a*)	(1$\bar{3}$2)	20	[230]	001	2·041	2·0210		
		½[011]			3$\bar{2}$0	0·290	0·2903	91·6	92·06
					3$\bar{2}$1	0·288	0·2889	84·0	83·84
					3$\bar{2}$$\bar{1}$	0·286	0·2860	100·0	100·19
					3$\bar{2}$2	0·280	0·2818	76·0	75·88
		⅛[121]			001	2·041	2·0210		
					3$\bar{2}$0	0·290	0·2905	91·6	90·69
					3$\bar{2}$1	0·288	0·2880	84·0	82·49
					3$\bar{2}$$\bar{1}$	0·286	0·2871	100·0	98·85
					3$\bar{2}$2	0·280	0·2801	76·0	74·60
4332	7(*b*)	(1$\bar{3}$2)	20	[110]	001	2·034	2·0210		
		½[011]			1$\bar{1}$0	0·679	0·6832	94·4	94·70
					1$\bar{1}$1	0·631	0·6317	112·5	112·85
					1$\bar{1}$2	0·546	0·5456	127·0	127·26
					1$\bar{1}$3	0·461	0·4611	137·8	137·72
		⅛[121]			001	2·034	2·0210		
					1$\bar{1}$0	0·679	0·6832	94·4	94·70
					1$\bar{1}$1	0·631	0·6317	112·5	112·85
					1$\bar{1}$2	0·546	0·5456	127·0	127·26
					1$\bar{1}$3	0·461	0·4611	137·8	137·72

countered; all could be indexed in a straightforward manner using the above matrices, which is a severe test of the proposed unit cells.

(*b*) *General observations*

All the samples were strikingly heterogeneous, as the summary in Table 4 shows. In addition, most diffraction patterns were complicated by the presence of the fine scale multiple twinning already referred to (*cf.* Fig. 1 of Bursill *et al.*, 1969). By carefully selecting areas containing only one orientation the effects of the latter have been practically eliminated in the patterns shown in Figs. 2 to 7. Areas containing only one *n* value were extremely rare; usually a parallel intergrowth of adjacent *n* values occurred. In the $(1\bar{2}1)_r$ mixtures these were immediately adjacent, *i.e.* $\Delta n=1$; *e.g.* Fig. 2 and 4(*b*) show $n=6,7$ and $n=9,10$ respectively. (N.B. The existence of $n=10(1\bar{2}1)_r$ had not previously been established.) In the $(1\bar{3}2)_r$ mixtures $\Delta n=2$ *always*: the mixtures $n=18,20$ and $n=20,22$ were frequently observed [Fig. 9(*a*) and (*b*)]. In contradiction with our preliminary assessment (Bursill *et al.*, 1969) a careful examination of the diffraction patterns from well-ordered samples has failed to establish unambiguous evidence for the existence of any $(1\bar{3}2)_r$ structure with an *odd* value of *n*. No phases were observed in the interval $1{\cdot}900<x<1{\cdot}938$ between $n=10(1\bar{2}1)_r$ and $n=16(1\bar{3}2)_r$. Fig. 9(*c*) shows that $n=9,10(1\bar{2}1)_r$ and $n=16(1\bar{3}2)_r$ coexist in the same area of a flake from sample 4.*

The diffraction patterns reveal a wide variation in the degree of ordering of the *CS* planes; the consequent effects range from sharp diffraction spots to continuous streaking along $\mathbf{g}\{1\bar{3}2\}_r$. Occasionally they are streaked parallel to both $\mathbf{g}\{101\}_r$ and $\mathbf{g}\{132\}_r$. In the

* *Note added in proof:* Subsequent work (to be published shortly) has changed this situation.

Table 4. *Phases observed in the various samples (all of which showed varying degrees of disorder)*

Sample No.	Estimated mean composition $\bar{x}$	$\bar{n}=1/(2-\bar{x})$	Observed *n* values $\{1\bar{2}1\}_r$	$\{1\bar{3}2\}_r$	Relevant Figure numbers (and *n* values)
1	1·96	25	–	20, ~25, >25	8(*a*) (disordered ~25)
2	1·945	18·2	–	16, 18, 20	5 (16), 7(*a*) (20), 7(*b*) (20)
3	1·936	15·6	9, 10	18, 20, ~25	6(*a*) (18), 6(*b*) (18), 9(*a*) (18, 20)
4	1·9268	13·5	7, 8, 9	16, 20, 22, 24	3 (8), 9(*c*) (9, 10, 16)
5	1·9247	13·5	6, 7, 8	20, 22	2 (6, 7), 9(*b*) (20, 22)
6	1·889	9	9, 10	16, 18, 20	4(*a*) (9), 4(*b*) (9, 10)

earlier paper (Bursill *et al.*, 1969) similar but much heavier streaking along $\mathbf{g}\{101\}_r$ was interpreted as possibly indicating the existence of a third family of structures, derived from rutile by regular *CS* planes parallel to {101}. We have since determined that the displacement vector at isolated {101} faults in fully oxidized rutile is $\mathbf{R}=\frac{1}{2}\langle 10\bar{1}\rangle$ (Bursill & Hyde, 1970). This is parallel to the fault plane, which is therefore an *APB* and not a *CS* plane. Consequently it does not change the stoichiometry of the crystal. We believe that these faults arise from the operation of the slip system $\frac{1}{2}\langle 10\bar{1}\rangle$ {101} (Ashbee & Smallman, 1963) as a result of the elastic stress during reduction, or possibly quenching.

5. Discussion

The observed electron diffraction patterns may be satisfactorily indexed by using the unit-cell parameters proposed in §2. It can be argued that other *CS* displacement vectors might give equally good agreement and, indeed, Table 3 shows that the *d* values and interplanar angles for $\frac{1}{6}[121]$ $(1\bar{3}2)$, (rutile) and $\frac{1}{2}[011]$ $(1\bar{3}2)$, (rutile) are barely distinguishable. However, the agreement between observed and calculated values is somewhat closer for the latter and, as mentioned earlier, $\frac{1}{2}[011]_r$ *is* the displacement vector at $(1\bar{3}2)_r$ *CS* planes when they occur singly or in groups. Finally, it is crystallochemically reasonable (while $\frac{1}{6}[121]_r$ is not). In direction and magnitude it corresponds very nearly to the edge of a $[TiO_6]$ octahedron in the rutile structure, and therefore allows a plane of empty oxygen sites to be refilled by translation of the adjacent oxygen plane while, at the same time, translating the titanium atoms from the normally occupied to the normally unoccupied octahedral interstices.

For the structures $4\leq n\leq 9(1\bar{2}1)_r$ Andersson & Jahnberg (1963) found that the observed unit-cell volumes were always slightly larger than the 'ideal' values. This they attributed to mutual repulsion of the close metal ions at the *CS* planes (in adjacent face-sharing octahedra). A similar expansion is to be expected for the $(1\bar{3}2)_r$ *CS* structures, but less pronounced because of the larger separation between the pairs of face-sharing octahedra, Selected area electron diffraction patterns are not sufficiently accurate to measure, or even confirm, this small expansion.

In samples 3, 4, 5 and 6 members of both the $(1\bar{2}1)_r$ and $(1\bar{3}2)_r$ families coexisted (Table 4). The highest value for $n(1\bar{2}1)_r$ and the lowest value for $n(1\bar{3}2)_r$ varies; they may well be temperature dependent.

The observed inhomogeneities may result from uptake of oxygen from the gas phase and/or unmixing during cooling. They prevent a definitive check of the proposed formula Ti_nO_{2n-1} for the $(1\bar{3}2)_r$ family bebecause it is not possible to make accurate estimates of the proportions of each of the several phases in a sample. But many specimens were studied from different portions of each sample and, with the exception of sample 6, they all showed a distribution of *n* values consistent with their independently determined mean compositions (Table 4). The most homogeneous was sample 2: it contained $n=16$, 18 and 20 and had a mean composition of $TiO_{1\cdot944}$ compared with the estimated $TiO_{1\cdot94-1\cdot95}$.

We are grateful for financial support provided by both the Australian Research Grants Committee and by AFOSR(SRC)-OAR through U.S.A.F. Grant No. AF-AFOSR-853-67. We would also like to acknowledge the provision of facilities by Dr L. N. D. Lucas and his staff at the Electron Microscopy Centre of this University, and assistance in sample preparation and analysis by Dr F. J. Lincoln and Mr R. R. Merritt of this department.

References

ANDERSON, J. S. & HYDE, B. G. (1967). *J. Phys. Chem. Solids*, **28**, 1393.

ANDERSSON, S. (1960). *Acta Chem. Scand.* **14**, 1161.

ANDERSSON, S. (1970). *The Chemistry of Extended Defects in Non-Metallic Solids*, Ed. L. EYRING and M. O'KEEFFE. Amsterdam: North-Holland.

ANDERSSON, S., COLLÉN, B., KUYLENSTIERNA, U. & MAGNÉLI, A. (1957). *Acta Chem. Scand.* **11**, 1641.

ANDERSSON, S. & JAHNBERG, L. (1963). *Ark. Kemi*, **21**, 413.

ASHBEE, K. H. G. & SMALLMAN, R. E. (1963). *Proc. Roy. Soc.* A **274**, 195.

BURSILL, L. A. & HYDE, B. G. (1970*a*). *Prcc. Roy. Soc.* A. In the press.

BURSILL, L. A. & HYDE, B. G. (1970*b*) *Phil. Mag.* In the press.

BURSILL, L. A., HYDE, B. G., TERASAKI, O. & WATANABE, D. (1969). *Phil. Mag.* **20**, 347.

EIKUM, A. & SMALLMAN, R. E. (1965). *Phil. Mag.* **11**, 627.

LANDUYT, J. VAN (1966). *Phys. Stat. Sol.* **16**, 585.

WYCKOFF, R. (1963). *Crystal Structures*, 2nd ed., Vol. I. New York: Interscience.